

CZECH UNIVERSITY OF LIFE SCIENCES PRAGUE

Faculty of Environmental Sciences



Optimization of Dual-Media Filters for Blue Energy

Bachelor Thesis

Supervisor: Ing. Roman Juras, Ph.D.

Consultant: Bárbara Vital, Ph.D.

Author of thesis: Fouad Farnisa

2023 CZU Prague

CZECH UNIVERSITY OF LIFE SCIENCES PRAGUE

Faculty of Environmental Sciences

BACHELOR THESIS ASSIGNMENT

Fouad Farnisa

Environmental Engineering

Thesis title

Optimization of Dual-Media Filters for Blue Energy

Objectives of thesis

Main Goal: Increasing the efficiency of the process by optimizing the pre-treatment.

Sub-goals:

- Increase flow velocity to achieve smaller footprint of the sand filters with the goal of running it at a high velocity.
- Try different configurations of media beds for better treatment.
- Optimizing the back-wash flow velocity for different media beds.

Methodology

Student will compute water flow velocities and pressure drop for both filters and stacks. Laboratory work also includes taking samples of the water going in & out of the system. Moreover, other parameters will be measured, such as Total Suspended Solids (TSS) and turbidity measurements. Results will be analysed in excel. Student will analyze stack performance by means of power output and pumping losses, he also do physical-chemical analysis of the treated and untreated water. With the best result student can figure out which configuration works best to reduce fouling and having a high-power output.

The proposed extent of the thesis

40 stran

Keywords

Electrodialysis, Blue Energy, stacks, ion exchange membrane, renewable energy

Recommended information sources

B. Vital, E.V. Torres, T. Sleutels, M.C. Gagliano, M. Saakes, H.V.M. Hamelers, Fouling fractionation in reverse electrodialysis with natural feed waters demonstrates dual media rapid filtration as an effective pre-treatment for fresh water, *Desalination* 518 (2021) 115277.

Expected date of thesis defence

2022/23 SS – FES

The Bachelor Thesis Supervisor

Ing. Roman Juras, Ph.D.

Supervising department

Department of Water Resources and Environmental Modeling

Electronic approval: 29. 3. 2023

prof. Ing. Martin Hanel, Ph.D.

Head of department

Electronic approval: 29. 3. 2023

prof. RNDr. Vladimír Bejček, CSc.

Dean

Prague on 29. 03. 2023

Acknowledgement:

I would like to thank Bárbara who gave me the opportunity to do an internship at Wetsus which gave me confidence in my professional scientific capabilities. In addition I would like to thank Wetsus Centre of Water Excellence for creating such an accepting and nurturing community for young professionals in the water technology field and to REDstack for providing the space to experiment on this new technology. I was first introduced to Roman when I went on a winter hydrological course in February 2022 and I was extremely pleased & grateful that he agreed to supervise my thesis despite it not being in his area of expertise. Furthermore I would like to send out much love to my sisters, friends, and colleagues who have helped me get to this point as I'm sure I could not have done it without their continuous support. I must also acknowledge that my internship which was the basis for this thesis was funded by an ERASMUS Traineeship which allowed me to do an internship for half a year in the Netherlands.

Declaration:

I hereby declare that I have independently elaborated the bachelor/final thesis with the topic of: Optimization of Dual-Media Filters for Blue Energy and that I have cited all of the information sources that I used in the thesis as listed at the end of the thesis in the list of used information sources.

I am aware that my bachelor/final thesis is subject to Act No. 121/2000 Coll., on copyright, on rights related to copyright, and on amendments of certain acts, as amended by later regulations, particularly the provisions of Section 35(3) of the act on the use of the thesis.

I am aware that by submitting the bachelor/final thesis I agree with its publication under Act No. 111/1998 Coll., on universities and on the change and amendments of certain acts, as amended, regardless of the result of its defence.

With my own signature, I also declare that the electronic version is identical to the printed version and the data stated in the thesis has been processed in relation to the GDPR. The student adds the date and place of the statement and signs it (Appendix No. 1).

In Prague, March, 29th, 2023

Signature:

Abstract:

The human population reached 8 billion in 2022 and continued to grow which caused an increased demand on agriculture, infrastructure and of course energy production. The human populations' need placed a huge strain on the environment in terms of deforestation, habitat disruption, and global climate change from which the effects became evident. To accommodate the needs of a growing population sustainable practices were necessary; the focus being on sustainable energy production. As the climate became less agreeable due to climate change renewable energy sources which depended on natural resources, such as hydroelectric dams and photovoltaic became negatively affected. Energy production through reverse electrodialysis (RED) was a novel form of energy production which gained traction as a promising renewable energy resource somewhat unaffected by climate variability. RED was a form of salinity gradient energy by which energy was captured from an energy potential formed by saline and freshwater on either side of a charged membrane. The main issue with *Blue Energy*, being membrane fouling, which increased resistance caused by scaling and formation of biofilm on membranes leading to a decrease in net power output. The aim of this thesis was to optimize the pre-treatment, thereby reducing fouling and increasing the amount of energy produced. Two alternate media bed configurations were used for the filtration system, namely activated filter media (AFM) and sand to compare filtration efficiency. Lab analyses were performed on the collected samples to analyze how much organic and inorganic matter made it through the filters; a metric which was used to determine filter efficiency. The primary results from the experiments & analyses were that AFM increased effluent quality for seawater whilst sand media removed more turbidity from freshwater. Sand filtration had an overall higher power density when compared to AFM, which highlighted the importance of high effluent quality of freshwater for RED.

Keywords:

Reverse Electrodialysis, Blue Energy, Activated Filter Media, Stacks, Ion Exchange Membranes, Renewable Energy, Salinity Gradient Energy, Fouling, Backwashing

Abstrakt:

Lidská populace dosáhla v roce 2022 8 miliard a nadále roste, což klade zvýšené nároky na zemědělství, infrastrukturu a samozřejmě výrobu energie. Potřeba lidské populace znamenala obrovskou zátěž pro životní prostředí, pokud jde o odlesňování, narušování biotopů a globální změny klimatu, jejichž důsledky se projeví. Aby bylo možné uspokojit potřeby rostoucí populace, bylo nutné používat udržitelné postupy; důraz byl kladen na udržitelnou výrobu energie. Vzhledem k tomu, že se klima v důsledku změny klimatu stalo méně příznivým, byly negativně ovlivněny obnovitelné zdroje energie, které závisely na přírodních zdrojích, jako jsou vodní přehradny a fotovoltaické elektrárny. Výroba energie pomocí reverzní elektrodialýzy (RED) byla novou formou výroby energie, která se prosadila jako slibný obnovitelný zdroj energie, na který nemá vliv proměnlivost klimatu. RED byla forma energie z gradientu slanosti, při níž se energie získávala z energetického potenciálu vytvořeného slanou a sladkou vodou na obou stranách nabitě membrány. Hlavním problémem modré energie bylo zanášení membrán, které zvyšovalo odpor způsobený usazováním vodního kamene a tvorbou biofilmu na membránách, což snižovalo čistý výkon tohoto nového obnovitelného zdroje energie. Cílem této práce bylo optimalizovat předúpravu, a tím snížit zanášení a zvýšit množství vyrobené energie. Pro filtrační systém byly použity dvě alternativní konfigurace filtračního lože, a to aktivovaná filtrační média (AFM) a písek, aby bylo možné porovnat účinnost filtrace. Na odebraných vzorcích byly provedeny laboratorní analýzy, aby se zjistilo, kolik organických a anorganických látek prošlo filtry; tento ukazatel byl použit k určení účinnosti filtru. Hlavními výsledky experimentů a analýz bylo, že AFM zvýšil kvalitu odpadní vody v mořské vodě, zatímco písková média odstranila více zákalu ze sladké vody. Písková filtrace měla ve srovnání s AFM mnohem vyšší hustotu výkonu, což zdůraznilo význam vysoké kvality odpadní vody pro RED.

Klíčová slova:

Reverzní elektrodialýza, modrá energie, aktivní filtrační média, komíny, iontoměničové membrány, obnovitelná energie, gradient slanosti, zanášení, zpětné proplachování

Abbreviations:

UN – United Nations

GHG – Greenhouse Gases

EU – European Union

PV – Photovoltaic

SGE – Salinity Gradient Energy

RED – Reverse Electrodialysis

ED – Electrodialysis

IEM – Ion-Exchange Membrane

CEM – Cation Exchange Membrane

AEM – Anion exchange Membrane

GAC – Granular Activated Carbon

AFM – Activated Filter Media

TOC – Total Organic Carbon

IC – Inorganic Carbon

TSS -Total Suspended Solids

NTU - Nephelometric Turbidity Unit

FSS – Fixed Solid Substances

VSS – Volatile Solid Substances

Table of Contents

1	Introduction.....	1
1.1	Current Energy Production with a focus on the Netherlands	1
1.2	Energy Production through Salinity Gradient Energy	3
1.3	Experiments on Blue Energy.....	5
1.4	Fouling & Mitigation.....	7
1.5	Why Blue Energy	8
2	Methodology	11
2.1	Filter Setup	11
2.1.1	Flow of Sand Filter System.....	13
2.1.2	Backwashing	14
2.2	Building Stack	14
2.3	TOC	16
2.4	TSS	16
2.5	Particle Size	18
2.6	Turbidity.....	18
3	Results and Discussion	19
3.1	Measured & Removed Turbidity.....	19
3.2	Pressure drop & Flow rate.....	21
3.3	Total organic carbon.....	23
3.4	Total suspended solids.....	24
3.5	Particle size.....	26
4	Conclusion	28
5	Bibliography	29
6	Table of figures.....	31
7	Appendix.....	34

1 Introduction

1.1 Current Energy Production with a focus on the Netherlands

The United Nations (UN) named ‘affordable and clean energy’ as the seventh of their seventeen sustainable development goals, which was an urgent call to action for all member countries (UN ©2015). Despite this call for action a 2022 report by the UN found that 733 million people lived without electricity, additionally financial aid to developing countries for renewables had decreased by \$13.8 billion over three years (UNSTATS ©2022). The European Union (EU), also aimed to transition the continent into the first climate-neutral society by 2050 (an economy with net-zero greenhouse gases (GHG) emissions), however data from EUROSTAT in 2020 showed that renewable energy sources only made up 17% of gross electricity consumption in the EU (EUROSTAT ©2020). This then begged the question, why half of the energy Sweden consumed came from renewables whilst Germany, Spain, France, and the Netherlands were below the European average.

The continued reliance on fossil fuels was attributed to an increased energy consumption, which grew rapidly over the past thirty years, and left countries with no other viable alternative (Newell et al., 2019). The global energy consumption which came from renewable energy was projected to increase from 15% in 2020 to 27% in 2050; whilst a 31% rise in natural gas was projected for the coming decade (U.S. Energy Information Administration ©2023). Coals share of the global energy use was on a projected decline through 2050 due to policies set by the EU and decreased investments in coal power plants; apart from countries such as India and China where the industry thrived (Newell et al., 2019). These projections highlighted the diversification of the global energy matrix and that older methods of energy production by fossil fuels were being phased out. But how could the production of renewable energy rise to meet the optimistic goals set by the UN and EU if most of the global energy market was projected to be dominated by liquid fuels for the foreseeable future. (U.S. Energy Information Administration ©2021)

This could be because many European countries lacked the necessary space or facilities to produce a substantial amount of their energy from renewable resources, so what were the alternatives for these countries if they intended on becoming a climate-

neutral society by 2050 (Li et al., 2019). For a low-lying country such as the Netherlands, with little land to spare for photovoltaic (PV)-fields and no options for hydroelectric dams, the possibilities for renewable energy sources in the country were slim (Rosenberg, 2009). Even though the country had minimal space for renewables, the Netherlands still invested into wind turbines and PV farms which contributed to a significant portion of the country's renewable energy production (De Jong, 2015). Clean energy production wasn't only in the interest of the nation or governing bodies, but also grassroot initiatives such as in the Dutch province of Friesland, which invested profits from the wind turbine farms back into their community (Oteman et al., 2017). This case highlighted the acceptance of renewable energy technologies in Friesland, but also the want to control where it gets installed (illustrated in **Figure 1**), and who profited from the installments.

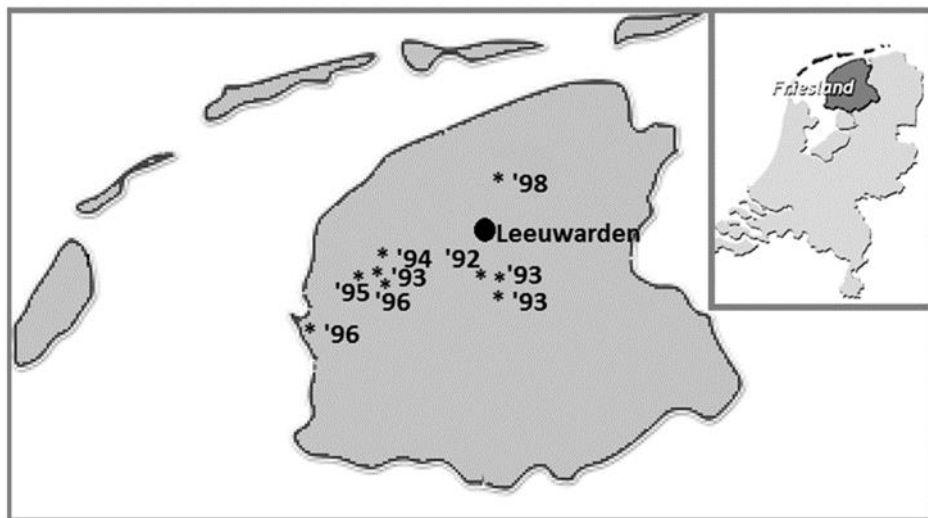


Figure 1: Wind turbine installments along with date of construction (Oteman et al., 2017).

Friesians had inhabited salt marshes in the northern region of the Netherlands since 700 BC and were the only people who occupied low lying regions of the country by constructing artificial dwelling mounds which protected their homes and herds from high tides & storm surges (Borger & Ligtenag, 1998). Due to sea level rise some of these mounds were raised to five meters in height, and catchment systems were built to collect rainwater for freshwater supply in their saline environment (Borger & Ligtenag, 1998). Water management in Friesland didn't stop there as from 1927 till 1933 a 32 km long, 7.25-meter-high Dijk was built to protect the Netherlands from the effects of the North Sea (Liu et al., 2012). This construction turned what used to be the saline South Sea, into a freshwater fed lake by the river IJ, which now inhabits

freshwater organisms such as *glykofyty glycopytes* (Westhoff & Sykora, 1979). This unique construction of fresh & seawater separated by less than a hundred meters of land sparked the interest of a company called REDstack BV (the Netherlands) which produced energy from the (semi-reversible) mixing of saline & freshwater (REDstack ©2023).

1.2 Energy Production through Salinity Gradient Energy

This method of energy production, called *Blue Energy*, was a novel form of salinity gradient energy (SGE), that used the theory of osmotic power, was first published in *Nature* by R.E. Pattle in 1954 (PATTLE, 1954). Osmosis being a physical phenomenon used since the early days of mankind, by which water moved from a solution with a low concentration of solvents to a high concentration (Cath et al., 2006). By the process of osmosis the solute difference across a semipermeable membrane created a high enough potential which caused the movement of water until equilibrium was reached illustrated in **Figure 2** (Cath et al., 2006). Pattle realised the potential created by fresh and saline waters on each side of a membrane could be converted into an electric potential (PATTLE, 1954).

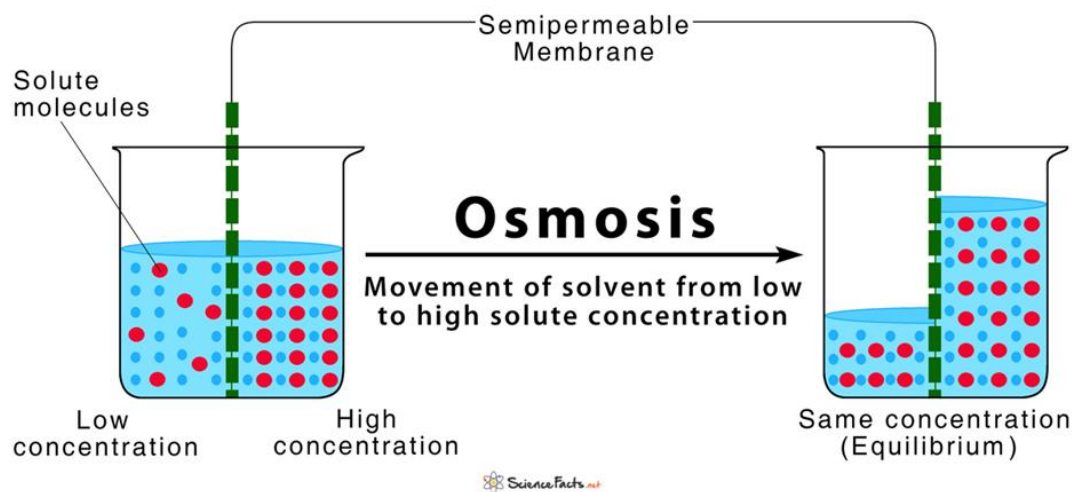


Figure 2: Simple sketch of osmosis in action (Science Facts ©2023).

SGE was then extensively researched from the 1970's to 80's, however due to the lack of membrane technology at the time, which was important for energy recovery, there were no practical applications of this technology (Norman, 1974). It was stated by (PATTLE, 1954), "that in addition to gravitational potential, natural

runoff in coastal areas had significant physical-chemical potential due to the salinity difference between fresh runoff (river mouths) and receiving salty reservoirs (seas and oceans)”. As a river flowed out into the sea, fresh and salt water combined, a natural, irreversible process from which no work was obtained, however energy could be recovered from the mixing process if it was done (somewhat) reversibly (Post, 2009). Pattle pointed out that many energy production methods existed using osmotic forces to obtain energy, however he was intrigued by a method dependent on the ionic nature of salt, which previously had been unmentioned in literature (PATTLE, 1954).

This process, now referred to as reverse electrodialysis (RED), generated electricity due to a salinity concentration differences; in contrast to electrodialysis (ED) which was widely used for the desalination of brackish water to drinking water (Tedesco et al., 2016). In both processes charged ion exchange membranes (IEM) prevented the transport of co-ions and allowed the transport of counter-ions (cations passing through anionic membranes & anions passing through cationic membranes) a side-by-side comparison of the processes was illustrated in **Figure 3** (Długołęcki et al., 2008). In ED an ionic current ran through the stack caused by voltage applied to electrodes at opposite ends of alternating IEM stacks which caused the feed stream to be separated and allowed the diluted stream to be harvested (Tedesco et al., 2016). In RED the stack was fed with a diluted and concentrated stream (fresh & seawater) to the alternating channels between the IEMs and conversely to ED the ion transport was caused due to a concentration difference (Tedesco et al., 2016).

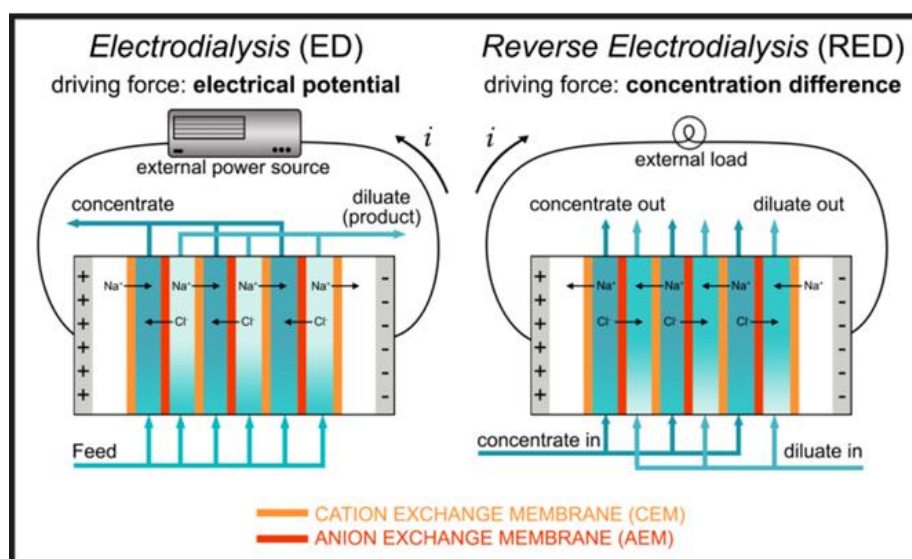


Figure 3: ED & RED design with i being the movement of energy in the process (Tedesco et al., 2016).

Electricity production from salinity gradients by RED occurred when an electric potential difference was created, and an electron could be transported from the anode to the cathode when an external circuit was connected, this generated power via redox reactions the same way a battery would when an external load was connected (Vital et al., 2021). If a current ran through the series of acidic and basic membranes which separated salt & freshwater, an electromotive force comparable to electrode polarization could be built up (PATTLE, 1954). Pattle stated, “this created a continuous supply of energy which would only need to be paused if the membranes required cleaning or replacing” the flow of energy illustrated in **Figure 4** (PATTLE, 1954). Pattle built this apparatus which consisted of a series of alternating membranes, incorporated with ion exchange resins, separating salt and freshwater which was being pumped in between the membranes through a series of holes and washers (PATTLE, 1954).

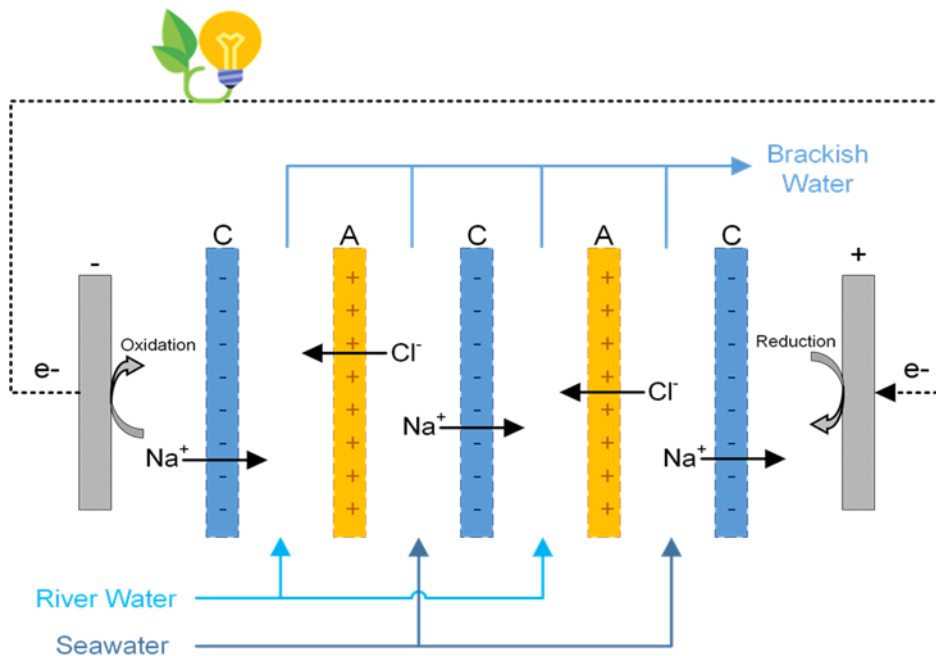


Figure 4: Scheme of RED (C. Simões, 2019).

1.3 Experiments on Blue Energy

Pattle designed this apparatus with membrane stacks of alternating cation exchange membranes (CEM) and anion exchange membranes (AEM) incorporated with ion-exchange resins which made them ion-selective therefore allowing this experiment to work (PATTLE, 1954). The salinity difference between the feed water

sources acted as an electromotive force in these RED systems, and ionic transport was aided by charge-selective IEMs (Post, 2009). Natural water sources with a salinity gradient, expected to feed this technology, were renewable salinity gradient resources that didn't affect the natural water cycle (Post, 2009). The first practical experiment on reverse electrodialysis was when professor Sidney Loeb used the energy recovered from SGE to power a heat engine, however even he criticized the large cost and suggested other forms of energy production (Loeb & Norman, 1975).

In laboratory trials, fake river and ocean waters were created using NaCl however the use of natural water sources had not been vastly studied thus far due to the many challenges that arose from using real waters in RED experiments (Rijnaarts et al., 2019). This made the research done for this thesis valuable as it was one of the first large-scale high-velocity experiment of *Blue Energy* where real waters were used. Previous studies showed that fouling on membranes could be attributed to organic, inorganic, microorganisms & extracellular polymeric substances, and particulate matter from seawater (Vital et al., 2021). Particulate matter had been classified into different size ranges from nanometers to 100 μ m, which contained organic and inorganic colloids such as: silt, clay, iron and aluminum compounds, and high molecular organic compounds (Rudolfs & Balmat, 1952). Particulate matter was small enough to block the pores of membranes and formed a top layer cake by microorganisms which grew on extra polymeric substances on the biofilm (Lim & Bai, 2003). This biofouling increased the pressure within the stack and reduced the power output due to the cake layer formation on membranes, more specifically the outer skin on this cake layer (shown in **Figure 5**) contributed to 90% of the overall filtration resistance (Guo et al., 2012).

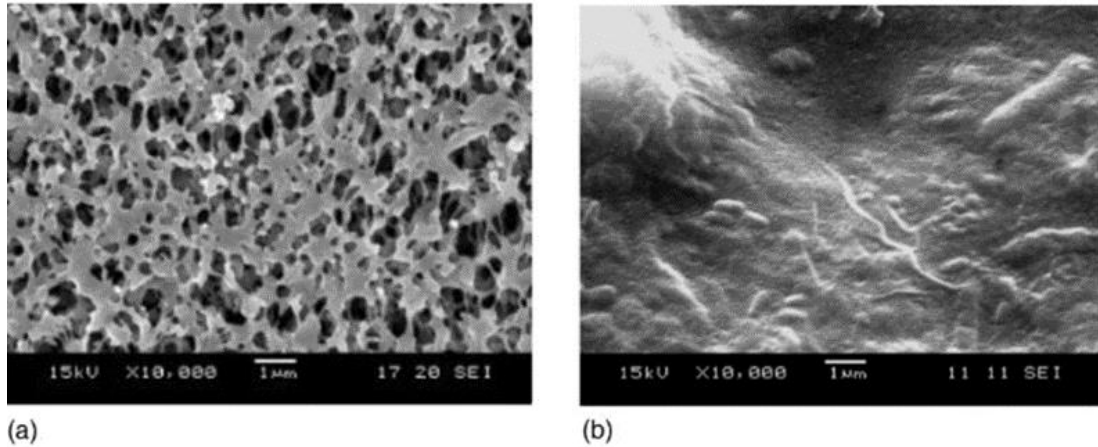


Figure 5: Images produced by SEM microscope (a) new membrane surface used in RED (b) membrane after experimental run showing pore blockage and biofouling (Lim & Bai, 2003).

1.4 Fouling & Mitigation

In freshwaters the positive charge of the AEM membranes in the stacks attracted the negatively charged humic substances which allowed them to get stuck to the membrane (Mikhaylin & Bazinet, 2016b). This caused some scientists working on SGE through RED to experiment with the application of polydopamine coating on the membranes, therefore increasing hydrophilicity which had antifouling potential (Vaselbehagh et al., 2014). Nano filtration had also been proven to remove smaller suspended particles, compared to dual media filtration, which could block the pore space of the membranes leading to a decrease in overall power density (Vital et al., 2021). Ultrafiltration, however was proven to have a lower total organic carbon (TOC) count and turbidity which created the best water quality compared to other filtration techniques (Ju et al., 2022). There were several antifouling measures performed such as periodic flow reversal (in which the sea & freshwater flow were switched) and air sparging (which involved injecting the stream of water with air) this technique removed colloidal fouling on the membranes (Vermaas et al., 2014).

Perhaps an obvious solution to fouling on the membrane surface would be to chemically treat the feed water or to physically clean the membranes using methods described in (Lin et al., 2010). However, during cleaning the set-up was non-operational, therefore taking time away from energy production, moreover the site where this experiment was run had strict regulations set by the government on the

quality of water which could be dumped into the Wadden Sea, which was a UNESCO site (UNESCO ©2009). Moreover, the point of Blue Energy was to have a low-cost renewable energy source that had minimal environmental effects, which would not be the case if chemicals were constantly being inputted into the system (Merino-Garcia & Velizarov, 2021). Although these filtering technologies were proven to be more effective in preventing fouling on the membranes, it added an additional step to the process which consumed more resources & time (Vital et al., 2023). This was why dual media filtration was best suited for this experiment as it was an environmentally friendly way to remove big particles which were more of a concern to power loss in the stacks (Cescon & Jiang, 2020).

In rapid dual-media filters fine sand and granular activated carbon (GAC) were typically used to physically remove impurities from influents due to sands ability to remove organic material (Environmental Protection Agency ©2020). Anthracite was used as a secondary media because it had a bigger grain size and was therefore able to remove bigger particulates before being ran through the sand (Sabiri et al., 2016). Activated filter media (AFM) was used instead of sand in one of the filters as it had been gaining more popularity and was proven to remove more turbidity and residual particles (Cescon & Jiang, 2020). AFM, made from recycled green bottles and was chosen in addition to anthracite as the synergetic effects of both filter medias was proven to improve the effluent quality of the water (Kim et al., 2021a). This was due to AFM's positive charge which in addition to being able to filter foulants in a similar manner to sand filtration was also able to attract negatively charged substances (Dryden Aqua ©2017).

1.5 Why Blue Energy

Renewable resources whether chemical, kinetic or thermal; harvested energy from the sun, wind, water or biomass and were therefore reliant upon unpredictable weather conditions (Ellabban et al., 2014). Global warming caused widespread changes in weather patterns which made extreme weather events such as storms, floods, and droughts even more frequent (U.S. EPA ©2022). In the case of PV, increased surface air temperature and wind velocity caused by global warming had a negative impact on power generation (Jerez et al., 2015). The same was true for hydroelectric dams which were directly affected by increased air temperature and

precipitation irregularities; in some cases, these irregularities caused droughts and disruptions in the hydrological cycle, which led to a decrease in power generation from hydroelectric dams (Dias et al., 2018). The renewable energy technologies which were meant to offset human-caused global warming became less efficient due to global warming therefore increasing reliance on fossil fuels.

Technological advancements had been made in many of these fields, considering that energy production cost from PV decreased by over 80% in the past decade (Apeh et al., 2022). The energy which could be harvested from these renewable energy sources was a promising step in the right direction, however recent findings showed that not all renewable resources had a positive effect on the environment (Hastik et al., 2015). Namely Hydroelectric dams caused river fragmentation which blocked migration routes directly affecting the life cycle of migratory species which led to extinction to some local species; this altered biotic interactions and ultimately caused imbalance in the ecosystem (Peluso et al., 2022). Furthermore, not all communities viewed these technologies positively as wind turbines decreased the property value of the areas on which they were installed and left the effected communities dissatisfied (Hastik et al., 2015).

After examining the data, a substantial gap was evident between the energy goals that the UN and EU had set and current energy consumption, social acceptance, and technological viability of renewable resources. A problem which was further exacerbated following the war in Ukraine which caused energy prices to raise globally (Tollefson, 2022). To tackle the issues at hand a non-combustion locally available alternative energy resource, that was renewable, and environmentally acceptable was suggested. While this concept seemed logical, it was not a particularly new, and one promising renewable and environmentally friendly energy source could be *Blue Energy*. This potential started to gain real traction when *Wetsus* institute started a *Blue Energy* theme in 2004 which created the spin-off company *REDstack* and almost a decade later the pilot plant on the Afsluitdijk was opened (REDstack ©2023). This exciting revelation even gained the interest of the Dutch King Willem-Alexander who conducted the grand opening in 2014 (REDstack ©2023).

Blue Energy could be a potential solution to the many problems listed, as it was a renewable energy source which was not really affected by the variability of nature, it was locally available, and was environmentally acceptable. For the reasons just

stated this topic was selected for this thesis, as this new technology was another way to capture an untapped sustainable energy resource to contribute to the worldwide growth in electricity consumption. To be more precise literature from the 70's indicated that globally there was an estimated 2.4-2.6 TW of energy that could be obtained based on the availability of freshwater in river deltas (Isaacs & Seymour, 1973). (Post, 2009) stated that this was sufficient to supply 80% of the world's electricity demand in 2009, which could've led to a potential 40% decrease in energy related GHG emissions. This was assumed from (Weinstein & Leitz, 1976) calculations that from each cubic meter of river water 2.3 MJ of energy could be extracted, this made the 30-km long Afsluitdijk in **Figure 6** comparable to a huge power dam of over 200 m high (assuming a level difference of only 1 m) (Post, 2009).

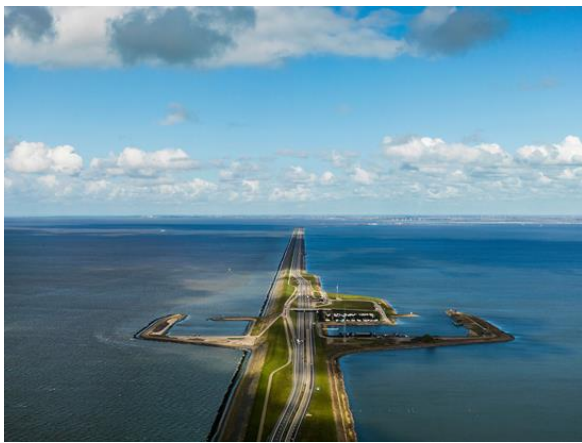


Figure 6: Aerial Photo of the Afsluitdijk (Siebe Swart ©2022).

2 Methodology

The location of the pilot plant where the experiments were run and conducted, was situated on the Afsluitdijk, more specifically Breezandijk, which separated the Wadden Sea and IJsselmeer (formerly known as Zuiderzee), shown in **Figure 7**.



Figure 7: Afsluitdijk in relation to North Sea, Wadden Sea, and Lake IJssel (NASA ©2021).

2.1 Filter Setup

The filtration system used for pre-treatment of waters was comprised of two main pumps, one used for the pumping of freshwater and the other for the pumping of salt water. The feed water ran through a 1 cm x 1 cm screen on the inlet of the pumping system and then a 5 mm coarse strainer prior to being pumped into four different filters through PVC pipes. The filtered water flowed out to the corresponding 50 L tanks which then ran to the stacks and the excess water overflow into one of the two 500 L tanks; a flow shown in **Figure 8**. Along the PVC pipes pressure and flow meters were installed to monitor pressure build-up which could be mitigated from one of the four controllers.

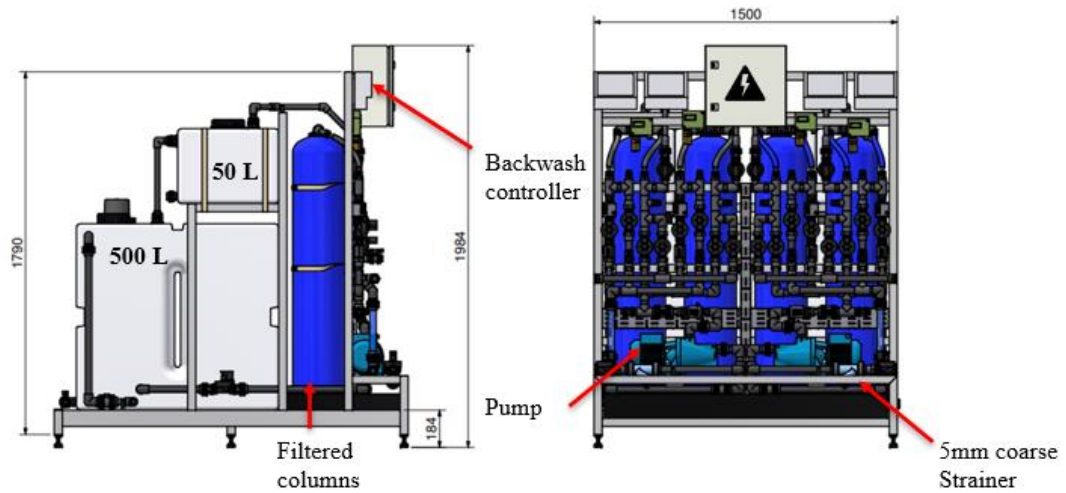


Figure 8: Adapted blueprint of automated sand filter from Hatenboer-Water BV (the Netherlands).

Inside the filters (two for seawater and two for freshwater) shown in **Figure 9** a dual-media bed was used to filter the water because it removed turbidity, organic substances, and suspended solids as low as 10-20 microns (Sabiri et al., 2016). In both sea/freshwater filters one filter was filled with 40 cm of anthracite (1.2–2.0 mm Ø) on top of 40 cm of sand (0.5–1.0 mm Ø). Anthracite (1.2–2.0 mm Ø) was also used in the second filter, but instead of sand, AFM *grade 1* (0.4-1.0 mm Ø) was used due to its ion selectivity and its similarity in size to sand (Dryden Aqua ©2017).

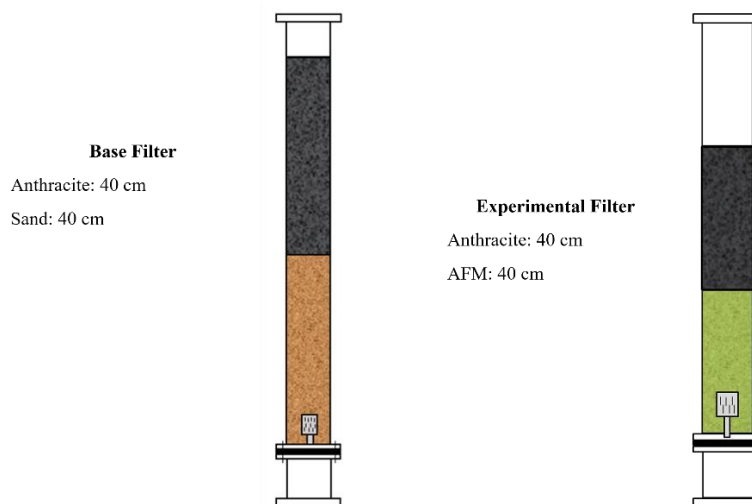


Figure 9: Dual-media filter bed in columns, designed by Hatenboer-water BV (the Netherlands).

2.1.1 Flow of Sand Filter System

Untreated water entered the system from pipes which pumped freshwater directly from the IJsselmeer and salt water from the Wadden Sea as illustrated in **Figure 10**. The water was then pumped through PVC pipes to the respective filter column, after which the filtered water then got up took by a pipe inside the filter column with a nozzle at the end, to prevent filter media from passing.



Figure 10: Water flow of the pilot plant on the Breezanddijk in relation to the Wadden Sea (REDstack ©2023).

Filtered water would be pumped to the stacks, a flow which was shown in **Figure 11** through tubes which were connected to a Masterflex L/S Digital drive. Each stack had freshwater and seawater pumped through it in a reverse flow system where freshwater would be pumped in through the bottom and pumped out through the top to ensure mixing with seawater. Electrolytes were also pumped into the stack using a Masterflex L/S Digital drive and was circulated within the stack before being pumped back into the electrolyte bottles. After the filtered sea/freshwater mixed and redox

reactions occurred within the stack the water was then pumped out of the system as brackish water and released into the Wadden Sea.

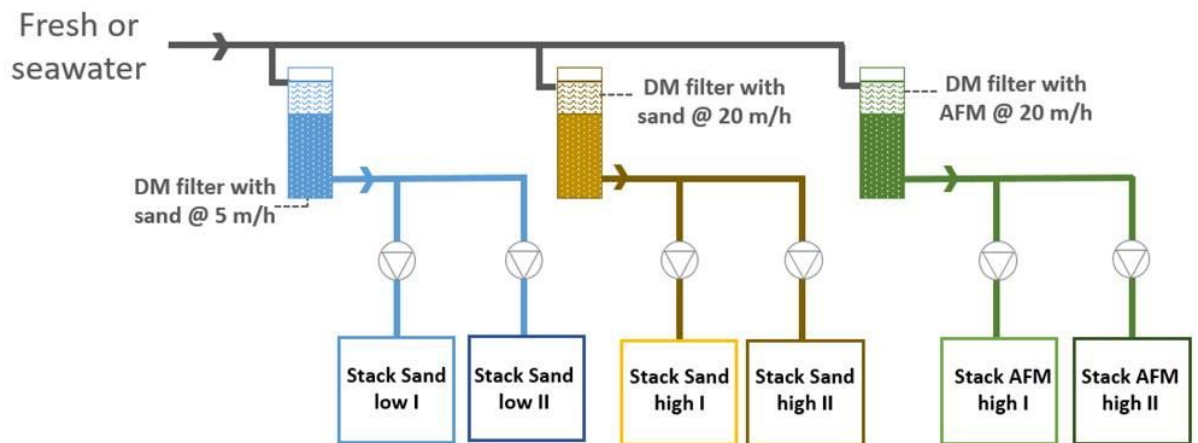


Figure 11: Stack flow feed for power generation (Vital et al., 2023).

2.1.2 Backwashing

The filters pressure loss would increase as the experiment ran on; due to fouling from the waters which were being filtered (Mesquita et al., 2019). This increase in pressure required the main pumps to use more energy to maintain the same flow, therefore decreasing the overall performance of the filters (Mesquita et al., 2019). As the experiment ran on there was a noticeable decrease in effluent quality (turbidity would be higher for example), this lower quality effluent was to be avoided from reaching the stacks. The excess water in the 500 L tanks were pumped upwards, which expanded and disrupted the filter bed and removed the foulants as they are less dense than the filter media (Mesquita et al., 2019). The controllers on each filter were set to backwash the filters every five hours automatically and the water would be allowed to run until the water coming out of the filters was visibly clear.

2.2 Building Stack

Stacks were built by fitting the metal frame of the stack onto the four threaded rods using nuts (washers were always placed in between the nuts & metal frames), the metal frame for the end plate was then placed above. One of the endplates along with a coarse mesh used to create a compartment for the electrodes were then placed above

the stack frame. The electrodes were in the end plates with a 500 μm silicon gasket used to create the electrolyte compartment, so that the electrolyte solution can circulate and be in contact with the electrodes. A one-sided profiled anode membrane was then placed on top of the silicon gasket followed by the cation side double-sided profiled membrane placed in an alternate direction. Membranes were profiled as per (Vermaas et al., 2011) method and placed in such a way that AEMs & CEMs were alternately stacked in a pile, forming eight cell pairs shown in **Figure 12**. A one-sided profiled cathode membrane was finally placed on top (maintaining the alternating pattern) along with another 500 μm silicon gasket to ensure the electrolyte solution could circulate. The membranes were then lined up after which the other endplate was placed on top, followed by the end plate frame, and was tightened to the metal rod using a torque wrench.

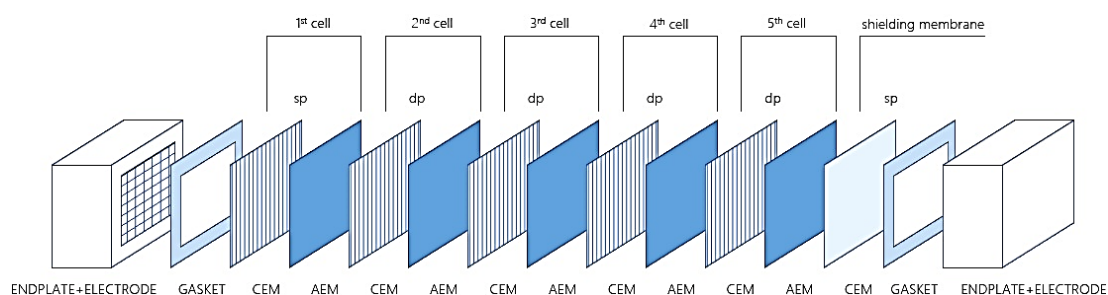


Figure 12: Stack membrane design using profiled membranes (Baron, 2022).

After the endplates were tightened the membranes got squished and protruded from the endplates, so it was necessary to shave them down using a circular cutting knife to make the membranes uniform with the endplates. Tereson RB IX was then placed on the corners of the membranes and onto the sides of the four side plates before they were screwed together using bolts, nuts, and washers. After the side plates were conjoined tar was squeezed through holes between the inner and outer O-rings using a syringe till the space was full, after which the holes were screwed shut, this process was done for all four side plates. The tar was left to sit for ten minutes, till it hardened, after which the other stack frame was tightened to the end and the stack was tested to make sure there was no leakage. If there was no leakage, electrolytes were also pumped through the stack using a Masterflex L/S Digital Drive and the stacks potential was tested using a potentiostat (Iviumstat, Ivium Technologies, Netherlands). The potentiostat was connected to a peripheral differential amplifier to measure voltage and

calculate the open circuit voltage, stack resistance and gross power density, using the same well established method as described in (Mikhaylin & Bazinet, 2016).

2.3 TOC

The samples for TOC were collected during the filtration of the samples of total suspended solids (TSS) using 50 ml falcons which were labeled according to the sample and placed in Büchner flask, after the filter had been rinsed with distilled water (DI). A rubber tube was inserted into the shackle of the funnel; this helped the sample flow into the falcon. The pump was then turned back on, and 30 mL of sample was poured through the filter and into the 50 ml falcon. The pump was then switched off and the funnel was then removed along with the vial, this process being repeated with all samples. For freshwater samples 10 mL was pipetted directly into a 20 mL TOC vial as well as 10 mL of mili-q creating 10x dilution. For seawater 0.909 mL of sample was pipetted into a 20 mL TOC vial in addition to 19.09 mL of mili-q, creating a 22x dilution. The samples were then analyzed by the analytical team of *Wetsus*.

2.4 TSS

TSS analysis were performed halfway through, and at the end of running the experiment, before backwashing. Samples were collected from filtered and unfiltered water in liter sampling bottles. Aluminum caps were then labeled on the bottom with a ballpoint pen with the name of sample, date, and name initials. Aluminum caps together with the respective filters were placed in the 105°C furnace for at least one hour to remove all air moisture from the filters, after which were placed in the desiccator for at least 15 minutes to cool down. Caps + filters were then weighed on an analytical scale and the values were recorded according to the given sample name. Then the area for the vacuum filtration was organized and all caps + filter and samples were placed nearby whilst the necessary glassware was collected.

A porcelain Büchner funnel was fitted on a Büchner flask with a rubber bung in between them; a pump was then connected to the Büchner flask through a tube to ensure that a vacuum was created as shown in **Figure 13**. One cap was chosen, and the dried filter was then placed on the Büchner funnel making sure that holes were covered by the filter, the pump was then turned on and DI was used to rinse the filter.

The corresponding sample measured out in the 500 mL graduated cylinder and was then poured through the wet filter making sure not to spill or overflow the sample. DI was then used to rinse the graduated cylinder and poured into the funnel to ensure that the entirety of the sample was ran through the filter, afterwhich DI was used to rinse the funnel to ensure that all particles passed through the filter.

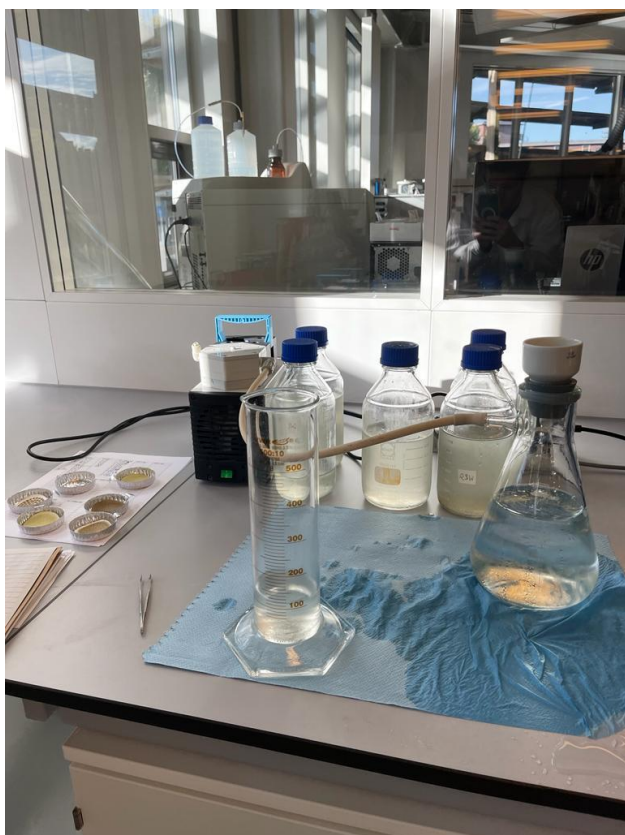


Figure 13: TSS experiment on treated waters

TSS was determined by pouring 200 mL of unfiltered sea or freshwater (250 mL of filtered freshwater or 700 mL of filtered seawater) from a 500 mL graduated cylinder through their respective $45\mu\text{m}$ borosilicate filter. The filter that had the sample filtered through it was then placed back in its corresponding aluminum cap & the amount of filtered was then recorded. The caps + filters were then placed in the 105°C furnace overnight, and the next day the filters + caps were placed in desiccator for 15 minutes to cool down and were then weighed and values recorded accordingly. Filters + caps were then placed in the furnace at 550°C ; the samples were then removed and placed in desiccator for 15 minutes after the program came to an end. The caps + filters were then weighed on the same analytical scale and values were then recorded accordingly.

The total suspended solids (TSS) measurements were calculated by these equations:

$$\text{TSS} = \frac{(m1 - m2) \times 1000}{(V0 \div 1000)} \quad \text{FSS} = \frac{(m3 - m2) \times 1000}{(V0 \div 1000)} \quad \text{VSS} = \text{TSS} - \text{FSS}$$

$m1$ - weight of filter with SS after drying in 105°C furnace [g]

$m2$ - weight of dry filter [g]

$m3$ - weight of filter with SS after drying in 550°C furnace [g]

$V0$ – filtrated volume [ml]

2.5 Particle Size

The remaining sample after TSS & TOC/IC analysis was used in determining particle size, which was determined using a Mastersizer 3000 (Malvern Panalytical, U.K.). Sample was poured into the *wet dispersion unit* until a value of 1-2% of obscuration was reached. After the program was run, the sample was tested five times and created averages based on the frequency of certain particle sizes (0.1, 1.0, 10.0, 100.0, 1000.0 μm). After obtaining and analyzing the results a *quick* clean was run in between different samples measurements and the program automatically generated graphs which could be used in samples analysis.

2.6 Turbidity

Turbidity was measured in Nephelometric Turbidity unit (NTU) with a HACH 2100N IS Turbidimeter hourly from unfiltered and filtered water. Sample was collected and poured until tube line. Silicone oil was then placed on glass tube and cleaned with a soft tissue to remove any fingerprints. The tube containing the water sample was then placed into Turbidimeter with the area where silicone oil was applied facing the laser. Values were collected and entered in an excel file to be used as a parameter of filtering quality. DI was used to clean the tube between different sample measurements.

3 Results and Discussion

The results from this experiment were collected from three-five hour runs of the automated sand filter machine, and from the lab analysis preformed on 28-09; 10-10; 02-11-2022, however all data used in this section were from 10-10-2022. Data presented in all graphs and bar charts (including appendix) were labelled as RFW, RSW, FW1, FW2, SW1, and SW2. Where RFW & RSW were the untreated water streams, FW1 & SW1 correlated to sand/anthracite filter columns, and FW2 & SW2 were AFM/anthracite filter columns.

3.1 Measured & Removed Turbidity

Peak turbidity did not follow any trend and was different from day to day as it was heavily reliant on the weather and water conditions. Treated water naturally being dependent on the untreated feed were several NTU's removed from the feed water. In all three runs the most variations occurred in untreated seawater with a $\pm 100-50$ NTU change just within one run on 02-11; untreated freshwater did not vary as much throughout the runs (only up to 50 NTU's max). Treated seawater turbidity consistently measured lower than freshwater turbidity, only on one occasion (02-11) where the measured untreated seawater turbidity was above 100 NTU. This demonstrated dual media filtration effectiveness in removing turbidity in seawater applications as on average they removed more than half of the turbidity from the feed water, outperforming treated freshwater.

It was also worth mentioning that in the first two hours where the untreated fresh/seawater were very similar the treated values had a difference of 5 NTUs, illustrated in **Figure 14**, highlighting the effectiveness of dual media filtration for seawater applications. AFM/anthracite pre-treatment had lower turbidity on average compared to sand/anthracite treatment for both fresh & seawater, highlighting the effectiveness of AFM pre-treatment. Turbidity was a good indicator of water quality and did show positive correlations with pressure drop in the filters, which led to flow rate drop during the experiment. It was also a great method to determine how effective the filters were by how much turbidity they were able to remove from the feed water. However, as the measurements were preformed manually, the recorded values could

be inaccurate as the values provided by the turbidimeter tended to jump around a lot and after a while NTU started to drop due to sedimentation.

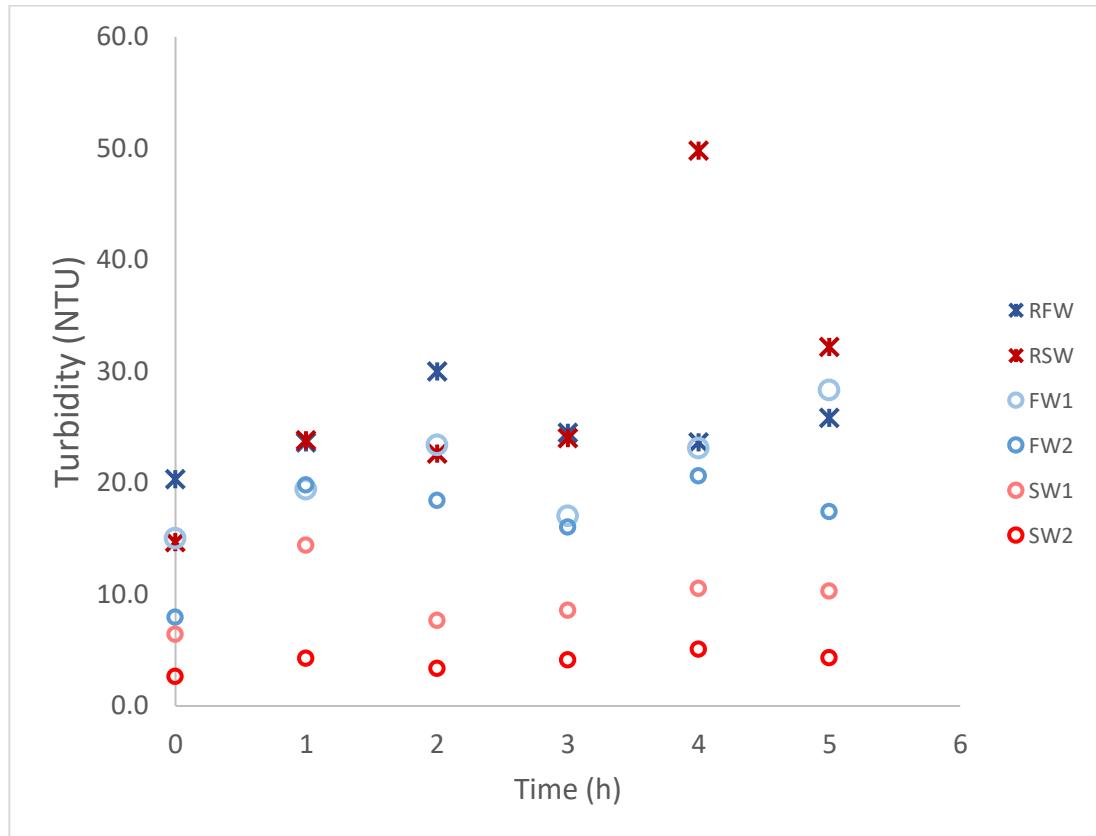


Figure 14: Measured turbidity from raw fresh/seawater and treated fresh/seawater.

On average FW1 removed 19%, FW2 removed 25.6%, SW1 removed 52%, and SW2 removed 66.6% of the turbidity from the untreated water. The seawater columns removed almost 36.5% more turbidity than freshwater columns which was huge considering the turbidity of the seawater samples. When comparing the efficiency of AFM and sand pre-treatment it was shown that AFM/anthracite columns for both sea & freshwater removed 11.1% more turbidity compared to sand/anthracite pre-treatment. This was due to the charge of the AFM, which was able to attract more particulates and aligned with (Kim et al., 2021) findings that made it a more effective pre-treatment for both applications. When plotted on a graph such as **Figure 15** it displayed what the filters removed in (NTU.m³) as the experiment progressed; however, to compare data on how much turbidity filters removed this data was turned into percentages and was averaged.

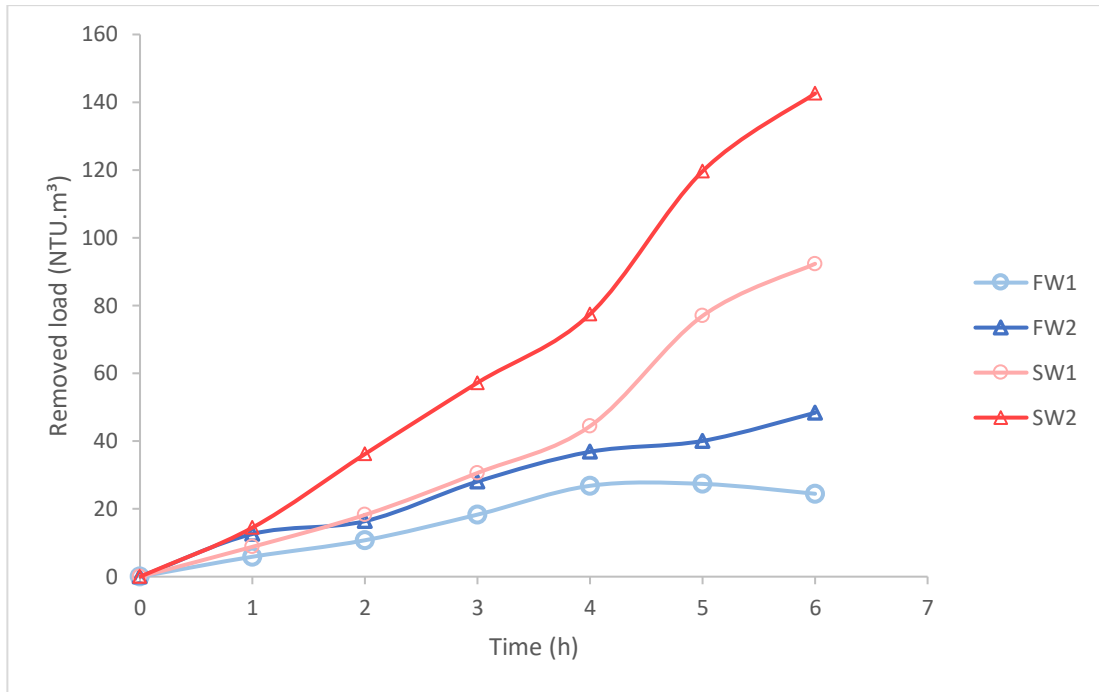


Figure 15: Removed turbidity was calculated in excel by subtracting the measured turbidity of the untreated water from the treated; multiplied by the flow rate, area of filter, and by how long the experiment had been ongoing to get the cumulative removed load.

Judging from the results it could be concluded that dual media filtration was most effective for seawater applications and using AFM instead of sand would significantly decrease effluent turbidity. Pre-treatment methods such as ultra/microfiltration could've removed more turbidity but as previously stated these methods would not provide the same velocity as dual media filtration therefore reducing energy production (Vital et al., 2021). It was also interesting to see the effect on treated water to a sudden decrease in water quality such as in 02-11 (an odd occurrence of treated seawater turbidity reaching 125 NTU). The filters were not as effective at removing turbidity as they would have been if the turbidity in the natural waters had been lower. When the turbidity of the natural waters were extremely high, such as on 02-11, they capped at 70% turbidity removal compared to hour 4 on 10-10 where the AFM/anthracite filter was able to remove 90% turbidity.

3.2 Pressure drop & Flow rate

Pressure for FW1 was consistently the highest of the four filter columns (as shown in **Figure 16**), which could be due to a problem in the sand filter; on 02-11 (a run where the recorded pressure was particularly high) FW1 reached 2000 mbars.

Flow velocities were maintained as high as possible (an example which was shown in **Figure 17**), as this was the goal of this thesis, and an increase in pressure resulted in a decrease in flow. As a result of the unusually high turbidity on 02-11 the flow reduced by 50%, which prevented water from reaching the stack, therefore reducing net energy production. The pressure became too high and as a countermeasure the column was backwashed as a mitigation measure to increase flow and the effluent quality which would reach the stack. Pressure build up was the most evident sign of high amount of fouling catchment in the filters apart from turbidity measured at different points of the system.

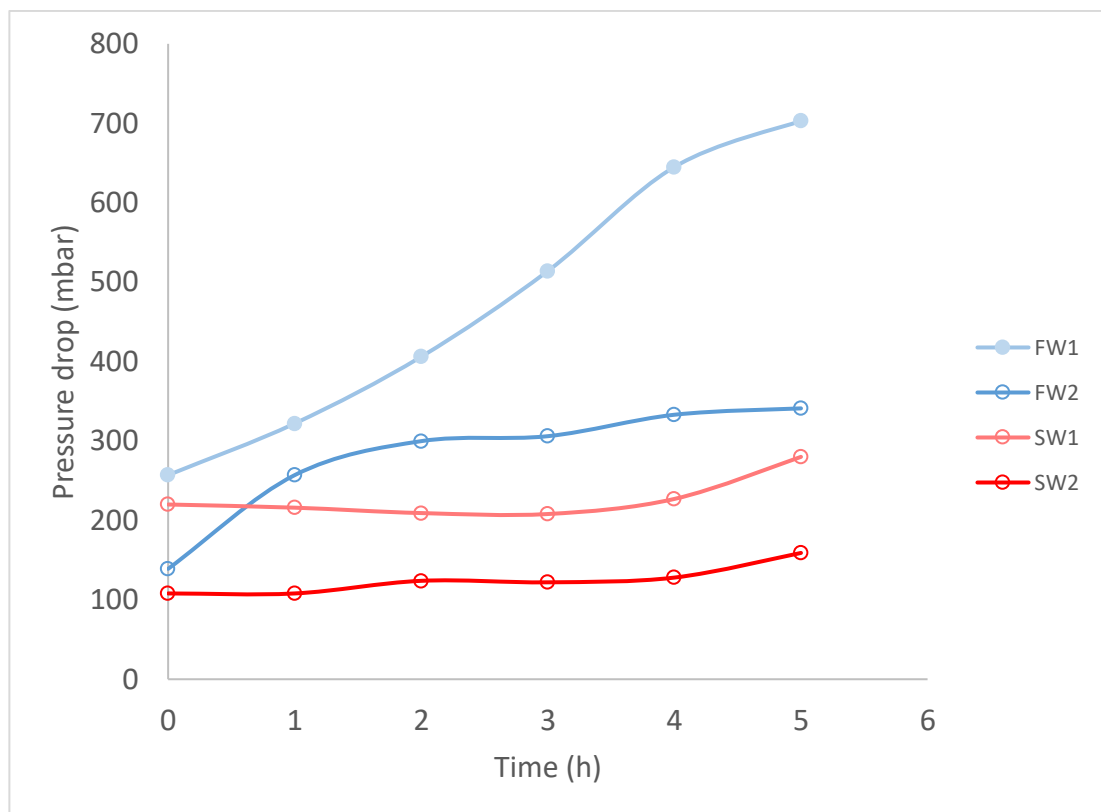


Figure 16: Measured pressure recorded manually from pressure meters connected to the *automated sand filter*.

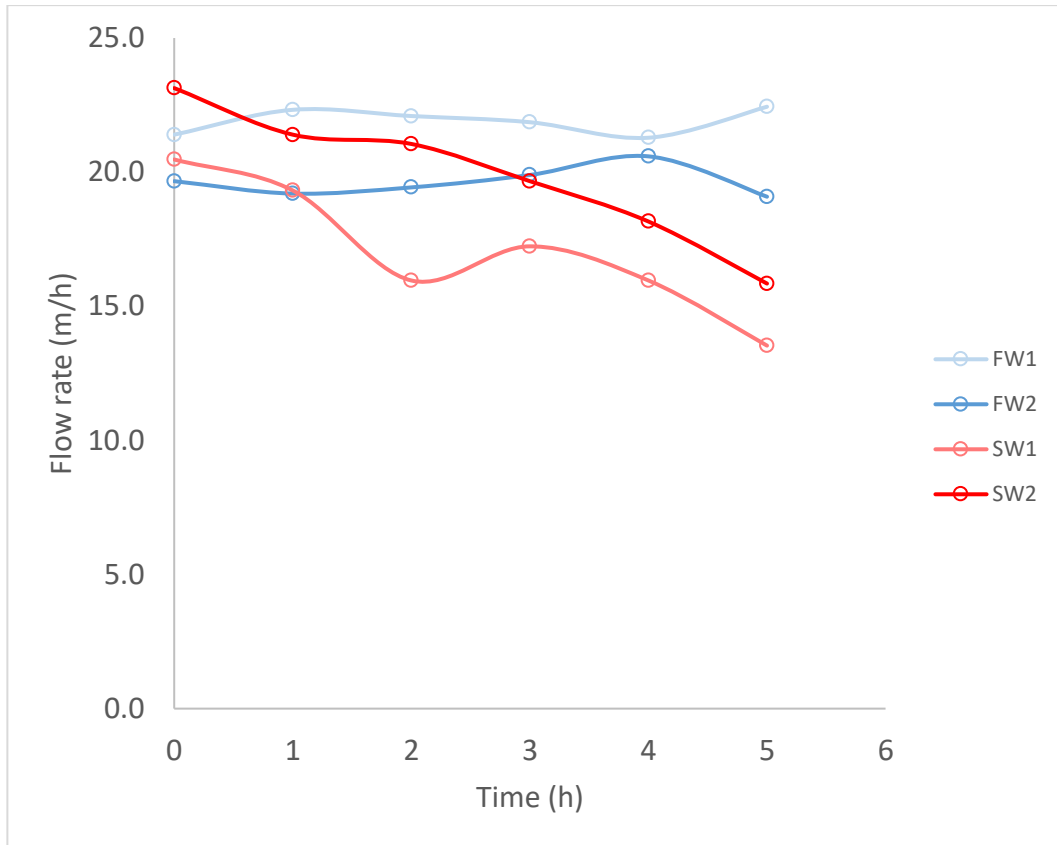


Figure 17: Measured flow recorded manually from flow meters on the *automated sand filter*.

For the optimization of backwash flow velocity the method used was trial and error based as if the backwash flow was too high you would visibly see filter media being backwashed. This was to be prevented so backwash flow was pushed to the limit which varied based on the filter column and media bed which you were backwashing. Finding the “goldilocks zone” for backwashing was fundamental for the operation of the *automated sand filter* as it increased the efficiency of the filters, which in turn decreased pressure and increased effluent quality. All of which was desired for increased energy production and minimal resistance from the stacks.

3.3 Total organic carbon

TOC values were obtained by subtracting the total carbon (TC) from the inorganic carbon (IC); this data showed the amount of carbon atoms tied up in organic compounds like in **Figure 18**. Comparing all treated and untreated runs TOC analysis was higher for AFM/anthracite pre-treatment compared to sand/anthracite filtration. It was also common throughout all three experimental runs for treated TOC values to be higher or like the untreated, this was probably caused by the remaining organic

compounds from previous runs. In (Kim et al., 2021) the synergetic effect of AFM & GAC were proven to reduce 97.4% of particulate fouling at a rate of 5 mL/min in a closed filtration system; additionally AFM removed 2 mg/L of TOC and improved the turbidity from 1.2 NTU to 0.12 NTU of wastewater.

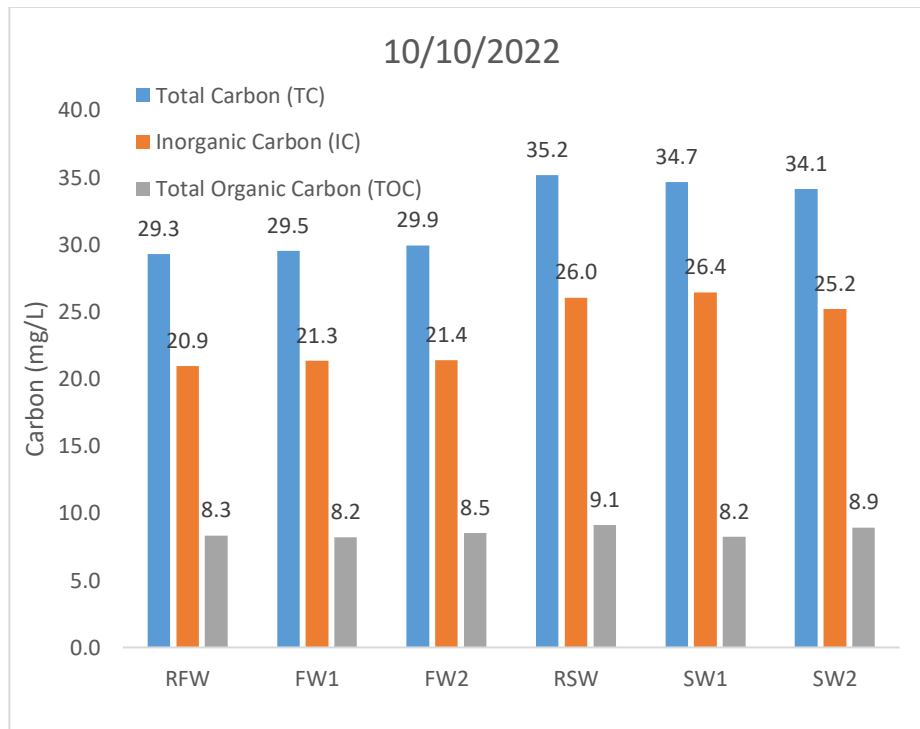


Figure 18: Lab analysis showing TC, IC, and TOC.

TOC measurements were excellent indicators of analyzing the water quality of untreated and treated waters; however could be affected by organic matter remaining in the filter columns from previous runs. Nevertheless, it was valuable information as it provided a clear view of matters present in the water prior to filtration and what remained post-treatment. TOC measurements were not, however correlated to turbidity as the highest TOC measurement recorded was on 28/09, where the turbidity was lowest.

3.4 Total suspended solids

TSS was comprised of two different measurements fixed suspended solids (FSS) and volatile suspended solids (VSS), being the difference between TSS and FSS, as shown in **Figure 19 & 20**. FSS were particles that did not burn in the 105°C oven, such as silt or clay, whilst VSS were the particles that did, such as organic matter. On

average untreated seawater did contain more TSS than freshwater, however treated freshwater contained much more TSS compared to its seawater counterpart. Seawater samples on the other hand contained much more FSS compared to the freshwater samples which had more of a balance between VSS & FSS.

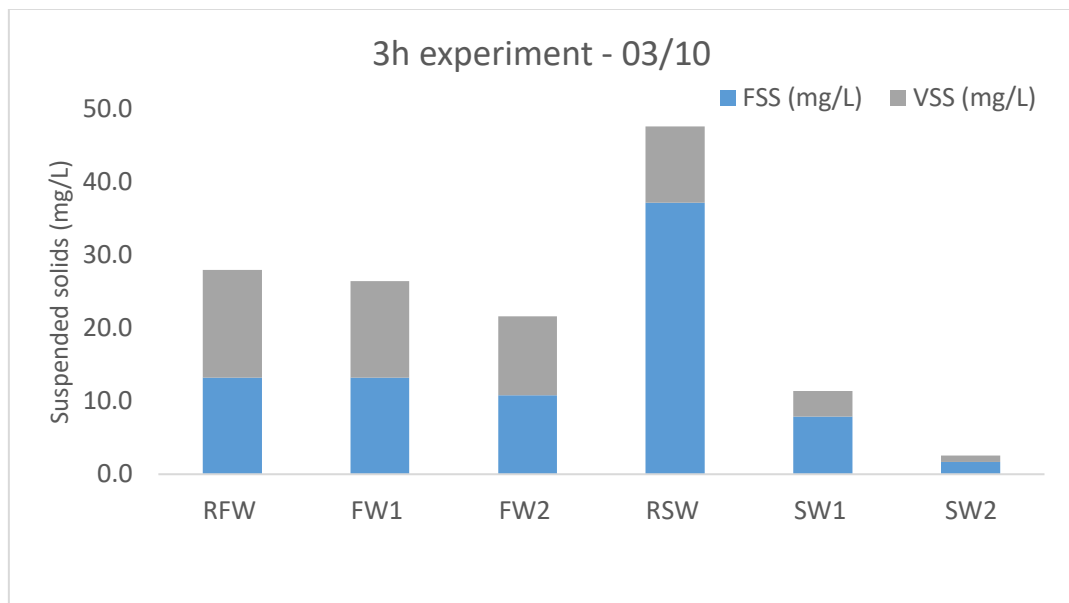


Figure 19: FSS & VSS measurements collected after 3 hours.

TSS showcased yet again how efficient dual-media filtration was for seawater, but also how it was lacking in some regards, compared to freshwater applications, which showed minimal decrease of suspended solids post-filtration. Based on the experimental runs chosen, and using TSS analysis as your only reference, it would be hard to determine whether AFM or sand had a better performance in removing suspended solids. This was because in some runs TSS was higher in treated waters than untreated and didn't show clear consistency in efficiency. Although, similarly to removed load, TSS analysis was yet another indicator of how effective dual-media filtration was at removing foulants in seawater.

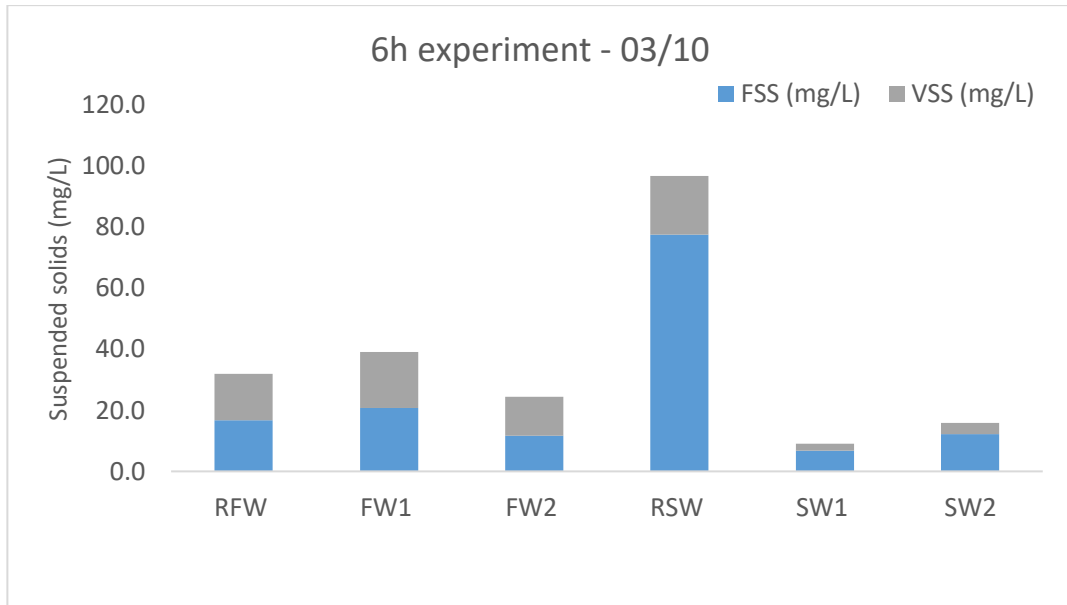


Figure 20: Measurements collected at end of experiment run prior to backwashing.

3.5 Particle size

The Mastersizer 3000 (Malvern Panalytical, U.K.) was able to measure the average diameter of particle size of particulate matter in the water. As shown in **Figures 21 & 22** freshwater filters removed particulates with a size density above 100 μ m, however the particle size density for sizes below 100 μ m did not decrease and in some cases increased. For seawater analysis there was more variation of particle sizes, and the treated water particle size density was higher for bigger particles compared to untreated. Comparing this to freshwater analysis of particle size (which had less of a range in particle sizes), the filters were able to reduce the density of particles above 100 μ m, but therefore causing an increase of particle size density in the range of 10-100 μ m. From the volume density it was evident that the dual-media filters were great at capturing particle sizes greater than 100 μ m however smaller particles passed through. In some runs the filters were able to remove particle size density in the range of 10-100 μ m but there was than an increase in particle sizes in the range of 100-1000 μ m.

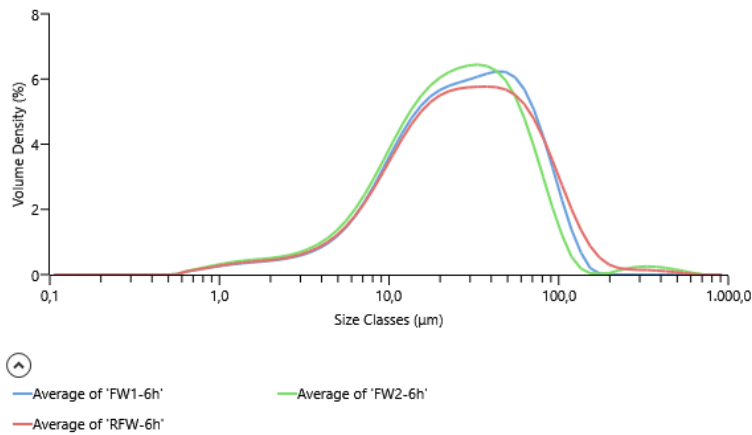


Figure 21: Average particle size diameter in freshwater collected at end of experiment run.

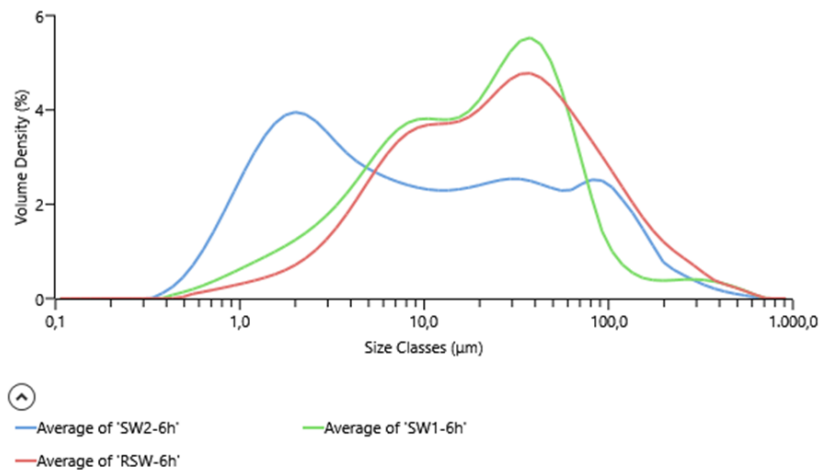


Figure 22: Particle size averages of salt water collected at the end of a six hour experiment.

Particle size was important because it offered great insight on what particle sizes were in the untreated water and what made it through to the treated water. Judging from the particle size analysis, the performance of the seawater filters was in part due to the vast range of particle sizes in seawater and the filters ability to remove a majority of the bigger particles. This supported results TSS results collected from the experiment and provided a clearer explanation of the results, particle size data also supported claims by (Vital et al., 2021).

4 Conclusion

Based on the findings it could be determined that dual-media pre-treatment with AFM and anthracite was more efficient at removing foulants. According to the weeklong run with the stacks the data clearly indicated that the stack which was being fed by high velocity sand/anthracite filter had almost two-times as much power density compared to the power density from all other stacks. This was shocking as it should be logical that if AFM/anthracite filters were able to produce higher effluent quality then the power density would be greater. This could be because sand/anthracite filtration removed more foulants from freshwater or because the stacks were faulty. This thesis had significant contribution to the field, as this was one of the first real-life experiments done on *Blue Energy* using real waters at high velocity. The results achieved could be used to further research done on *Blue Energy* as well as dual-media filtration as a pre-treatment for *Blue Energy*, and other applications of AFM as a form of pre-treatment. This results from this experiment showcased the effectiveness of dual media filtration on seawater and highlighted that it may not be the best pretreatment for freshwater applications. SGE still requires more research before it could be considered for a substitute for fossil fuels, however there isn't a "one solution fits all" when it comes to energy production or combating climate change. Although this thesis main focus was not on the power production from RED it did showcase the fouling from different pre-treatment methods which would negatively effect the net power density produced by the stacks in RED. The best way being an effective pre-treatment and done in environmentally friendly way which this thesis would be a great reference on which pre-treatment would be best for high-scale *Blue Energy* production.

5 Bibliography

- Dryden, H. T. (2007). Drinking water: Improving sand filter performance. *Filtration & Separation*, 44(5), 22–25. [https://doi.org/10.1016/S0015-1882\(07\)70144-1](https://doi.org/10.1016/S0015-1882(07)70144-1)
- Kim, H., Choi, Y., Lee, S., Lee, K. B., Jung, K. W., & Choi, J. W. (2021). Pretreatment for capacitive deionization: Feasibility tests using activated filter media and granule activated carbon filtration. *Journal of Industrial and Engineering Chemistry*, 93, 253–258. <https://doi.org/10.1016/J.JIEC.2020.10.001>
- Mesquita, M., de Deus, F. P., Testezlaf, R., da Rosa, L. M., & Diotto, A. V. (2019). Design and hydrodynamic performance testing of a new pressure sand filter diffuser plate using numerical simulation. *Biosystems Engineering*, 183, 58–69. <https://doi.org/10.1016/j.biosystemseng.2019.04.015>
- Mikhaylin, S., & Bazinet, L. (2016). Fouling on ion-exchange membranes: Classification, characterization and strategies of prevention and control. *Advances in Colloid and Interface Science*, 229, 34–56. <https://doi.org/10.1016/j.cis.2015.12.006>
- Sabiri, N.-E., Monnier, E., Raimbault, V., Massé, A., Séchet, V., & Jaouen, P. (2016). *Environmental Technology ISSN: (Print) (Online) Journal homepage: https://www.tandfonline.com/loi/tent20 Effect of filtration rate on coal-sand dual-media filter performances for microalgae removal Effect of filtration rate on coal-sand dual-media filter performances for microalgae removal.* <https://doi.org/10.1080/09593330.2016.1193224>
- Vermaas, D. A., Saakes, M., & Nijmeijer, K. (2011). Power generation using profiled membranes in reverse electrodialysis. *Journal of Membrane Science*, 385–386, 234–242. <https://doi.org/10.1016/j.memsci.2011.09.043>
- Vital, B., Torres, E. V., Sleutels, T., Gagliano, M. C., Saakes, M., & Hamelers, H. V. M. (2021). Fouling fractionation in reverse electrodialysis with natural feed waters demonstrates dual media rapid filtration as an effective pre-treatment for fresh water. *Desalination*, 518, 115277. <https://doi.org/10.1016/j.desal.2021.115277>

6 Table of figures

Figure 1: Wind turbine installments along with date of construction (Oteman et al., 2017).	2
Figure 2: Simple sketch of osmosis in action (Science Facts ©2023).....	3
Figure 3: ED & RED design with i being the movement of energy in the process (Tedesco et al., 2016).....	4
Figure 4: Scheme of RED (C. Simões, 2019).	5
Figure 5: Images produced by SEM microscope (a) new membrane surface used in RED (b) membrane after experimental run showing pore blockage and biofouling (Lim & Bai, 2003).....	7
Figure 6: Aerial Photo of the Afsluitdijk (Siebe Swart ©2022).	10
Figure 7: Afsluitdijk in relation to North Sea, Wadden Sea, and Lake IJssel (NASA ©2021).	11
Figure 8: Adapted blueprint of automated sand filter from Hatenboer-Water BV (the Netherlands).....	12
Figure 9: Dual-media filter bed in columns, designed by Hatenboer-water BV (the Netherlands).....	12
Figure 10: Water flow of the pilot plant on the Breezendijk in relation to the Wadden Sea (REDstack ©2023).....	13
Figure 11: Stack flow feed for power generation (Vital et al., 2023).	14
Figure 12: Stack membrane design using profiled membranes (Baron, 2022).....	15
Figure 13: TSS experiment on treated waters	17
Figure 14: Measured turbidity from raw fresh/seawater and treated fresh/seawater.	20
Figure 15: Removed turbidity was calculated in excel by subtracting the measured turbidity of the untreated water from the treated; multiplied by the flow rate, area of filter, and by how long the experiment had been ongoing to get the cumulative removed load.....	21
Figure 16: Measured pressure recorded manually from pressure meters connected to the <i>automated sand filter</i>	22
Figure 17: Measured flow recorded manually from flow meters on the <i>automated sand filter</i>	23
Figure 18: Lab analysis showing TC, IC, and TOC.....	24
Figure 19: FSS & VSS measurements collected after 3 hours.....	25

Figure 20: Measurements collected at end of experiment run prior to backwashing.	26
Figure 21: Average particle size diameter in freshwater collected at end of experiment run.	27
Figure 22: Particle size averages of salt water collected at the end of a six hour experiment.....	27
Figure 23: Turbidity measured on 02.11.2022.....	34
Figure 24: Pressure drop collected on 02.11.2022.....	34
Figure 25: Measured flow rate on 02.11.2022	35
Figure 26: Filters removed load on 02.11.2022	35
Figure 27: TSS measurement collected on 02.11.2022.....	36
Figure 28: TSS measurement after five hours from experimental run on 02.11.2022	36
Figure 29: TOC measurement.....	37
Figure 30: Particle size averages for fresh water measured on 02.11.2022.....	37
Figure 31: Particle size averages for sea water measured on 02.11.2022.....	38
Figure 32: Measured turbidity for treated & untreated water collected on 28.09.2022	38
Figure 33: Measured pressure over experimental run on 28.09.2022.....	39
Figure 34: Measured flow collected on 28.09.2022.....	39
Figure 35: Removed load collected on 28.09.2022 calculated in excel.....	40
Figure 36: TOC measured from samples at end of experiment run.....	40
Figure 37: TSS measurement performed three hours after start of experiment on 28.09.2022.....	41
Figure 38: TSS performed at end of experiment on 28.09.2022.....	41
Figure 39: Average particle size of particulates in fresh water samples collected on 28.09.2022.....	42
Figure 40: Particulate matter size of treated & untreated salt water samples collected on 28.09.2022.....	42
Figure 41: Power potential from stacks measured on (Iviumstat, Ivium Technologies, Netherlands) Stack 1 & 2 received sand filtered water at high velocity, Stack 3 & 4 received AFM filtered water at high velocity, and Stack 5 received sand filtered water at low velocity.....	43

Figure 42: Total resistance in stacks measured on (Iviumstat, Ivium Technologies, Netherlands) Stack 1 & 2 received sand filtered water at high velocity, Stack 3 & 4 received AFM filtered water at high velocity, and Stack 5 received sand filtered water at low velocity..... 44

Figure 43: Power density from Stack 1 & 2 which received sand filtered water at high velocity, Stack 3 & 4 which received AFM filtered water at high velocity, and Stack 5 which received sand filtered water at low velocity..... 45